Review Article

Plaque imaging with CT—a comprehensive review on coronary CT angiography based risk assessment

Márton Kolossváry, Bálint Szilveszter, Béla Merkely, Pál Maurovich-Horvat

MTA-SE Cardiovascular Imaging Research Group, Heart and Vascular Center, Semmelweis University, Budapest, Hungary

Contributions: (I) Conception and design: All authors; (II) Administrative support: P Maurovich-Horvat; (III) Provision of study material or patients: All authors; (IV) Collection and assembly of data: All authors; (V) Data analysis and interpretation: M Kolossváry; (VI) Manuscript writing: All authors; (VII) Final approval of manuscript: All authors.

Correspondence to: Pál Maurovich-Horvat, MD, PhD, MPH. 68, Városmajor Street, 1122 Budapest, Hungary. Email: p.maurovich.horvat@mail.harvard.edu.

Abstract: CT based technologies have evolved considerably in recent years. Coronary CT angiography (CTA) provides robust assessment of coronary artery disease (CAD). Early coronary CTA imaging—as a gate-keeper of invasive angiography—has focused on the presence of obstructive stenosis. Coronary CTA is currently the only non-invasive imaging modality for the evaluation of non-obstructive CAD, which has been shown to contribute to adverse cardiac events. Importantly, improved spatial resolution of CT scanners and novel image reconstruction algorithms enable the quantification and characterization of atherosclerotic plaques. State-of-the-art CT imaging can therefore reliably assess the extent of CAD and differentiate between various plaque features. Recent studies have demonstrated the incremental prognostic value of adverse plaque features over luminal stenosis. Comprehensive coronary plaque assessment holds potential to significantly improve individual risk assessment incorporating adverse plaque characteristics, the extent and severity of atherosclerotic plaque burden. As a result, several coronary CTA based composite risk scores have been proposed recently to determine patients at high risk for adverse events. Coronary CTA became a promising modality for the evaluation of functional significance of coronary lesions using CT derived fractional flow reserve (FFR-CT) and/or rest/dynamic myocardial CT perfusion. This could lead to substantial reduction in unnecessary invasive catheterization procedures and provide information on ischemic burden of CAD. Discordance between the degree of stenosis and ischemia has been recognized in clinical landmark trials using invasive FFR. Both lesion stenosis and composition are possibly related to myocardial ischemia. The evaluation of lesion-specific ischemia using combined functional and morphological plaque information could ultimately improve the diagnostic performance of CTA and thus patient care. In this review we aimed to summarize current evidence on comprehensive coronary artery plaque assessment using coronary CTA.

Keywords: Coronary CT angiography (coronary CTA); risk assessment; coronary artery disease (CAD)

Submitted Sep 21, 2016. Accepted for publication Dec 08, 2016.
doi: 10.21037/cdt.2016.11.06
View this article at: http://dx.doi.org/10.21037/cdt.2016.11.06

Introduction

After the first description of CT angiography (CTA) in 1992 (1,2), further technological advances, such as: more powerful X-ray tubes, faster gantry rotation times, multiple parallel detector rings and decreased slice thickness (3,4) were introduced, that allowed the visualization of the coronary arteries (5). Coronary CTA has emerged as a non-invasive alternative to invasive coronary angiography (ICA) for the diagnosis of obstructive coronary artery disease (CAD). With its excellent sensitivity and negative predictive value (6,7), coronary CTA is a robust diagnostic test to rule out severe coronary stenosis and is widely used as a "gate-keeper" for ICA (8,9). Nevertheless, modern CT scanners

allow not only the visualization of the coronary lumen as ICA, but also the vessel wall, granting non-invasive analysis of atherosclerosis itself. This unique property of coronary CTA holds many advantages for patient risk stratification, that other non-invasive tests do not. Coronary CTA is currently also the only non-invasive imaging modality for the evaluation of non-obstructive CAD.

Cadaver studies of acute coronary syndrome (ACS) patients have shown that plaque morphology plays a crucial role in developing ACS (10). With around half of plaque ruptures occurring at lesion sites with smaller than 50% diameter stenosis (11-13), plaque morphology assessment seems equally as important as stenosis assessment. Furthermore, recent studies have indicated that coronary plaque burden also has a substantial effect on all-cause mortality (14,15). Due to its volumetric imaging capabilities coronary CTA depicts around twice as many atherosclerotic lesions as ICA (16,17), thus risk assessment based on atherosclerotic plaque burden may be a unique ability of coronary CTA.

Our objective was to review the current literature on stenosis, qualitative plaque morphology, plaque burden and composite plaque burden score assessment using coronary CTA, and examine their effect on patient morbidity and mortality.

Plaque morphology assessment with coronary CTA

Atherosclerosis is initiated by deposition of low density lipoproteins (LDL) in the intima. With oxidation of the lipids, an inflammatory response is triggered, which is characterized by macrophages engulfing oxidized LDL particles, thus becoming foam cells (18). Poorly understood genetic and environmental factors propagate inflammation resulting in further deposition of lipids, deterioration of the extracellular matrix and cell death (19). These processes lead to distinct plaque morphologies, which have been identified on histological samples, and have brought forward the concept of the vulnerable plaque (20). With submillimeter isotropic resolution coronary CTA is capable of imaging not only the lumen, but also the coronary wall, thus allowing non-invasive morphological assessment of coronary atherosclerosis.

Plaque composition

Coronary plaques can be classified as being: non-calcified, partially calcified or calcified based on the amount of calcium in the lesion (*Figure 1*) (21). Large multicenter cohorts such as the COronary CT Angiography EvaluatioN For Clinical Outcomes: An InteRnational Multicenter (CONFIRM) registry (22), investigated the prognostic value of plaque composition on all-cause mortality. Based on 17,793 suspected CAD patients' 2-year survival data, the number of segments with partially calcified or calcified plaque had a significant effect on mortality (hazard ratios: non-calcified: 1.00, P=0.90; partially calcified: 1.06, P≤0.0001; calcified: 1.08, P≤0.0001). After adjusting for clinical factors, none of the plaque components improved the diagnostic accuracy of the model (non-calcified: P=0.99; partially calcified: P=0.60; calcified: P=0.10) (15). Hadamitzky *et al.* found similar results when investigating the prognostic effect of plaque composition on 5-year mortality rate based on suspected CAD patients. After adjusting of clinical risk based on the Morise score (23), only the number of segments with calcified plaques improved significantly the diagnostic accuracy of the model (non-calcified: P=0.083; partially calcified: P=0.053, calcified: P=0.041) (24). Dedic *et al.* found similar results in a different patient population. When investigating the effects of different plaque components of non-culprit lesions on future major adverse cardiac events (MACE) in ACS patients, they found none of the plaque types to have a significant impact on future MACE rates (hazard ratios: non-calcified: 1.09, P=0.11; partially calcified: 1.11, P=0.35; calcified: 1.11, P=0.15) (25). Interestingly Nance *et al.* found very different results when analyzing 458 patients' data, who presented to the emergency room with acute chest pain but based on ECG and serum creatinine had inconclusive results and thus underwent coronary CTA. All patients had low to intermediate risk for CAD. After a follow-up of 13 months, they split the patients into three groups: only non-calcified plaques; exclusively calcified plaques; any partially calcified plaque or both non-calcified and calcified plaques. After adjustment for clinical characteristics and Ca-score they found the following hazard ratios: 57.64 for non-calcified, 55.76 for partially calcified and 26.45 for patients with solely calcified plaques (26). The difference compared to other studies might be due to the different methodological approach used. While previously mentioned papers examined the effect of plaque composition on a segment based level incrementally, giving the hazard ratio of an increase in the number of segments with a given plaque type, Nance *et al.* reported the results on a patient based level dichotomized, giving the hazard ratio of having

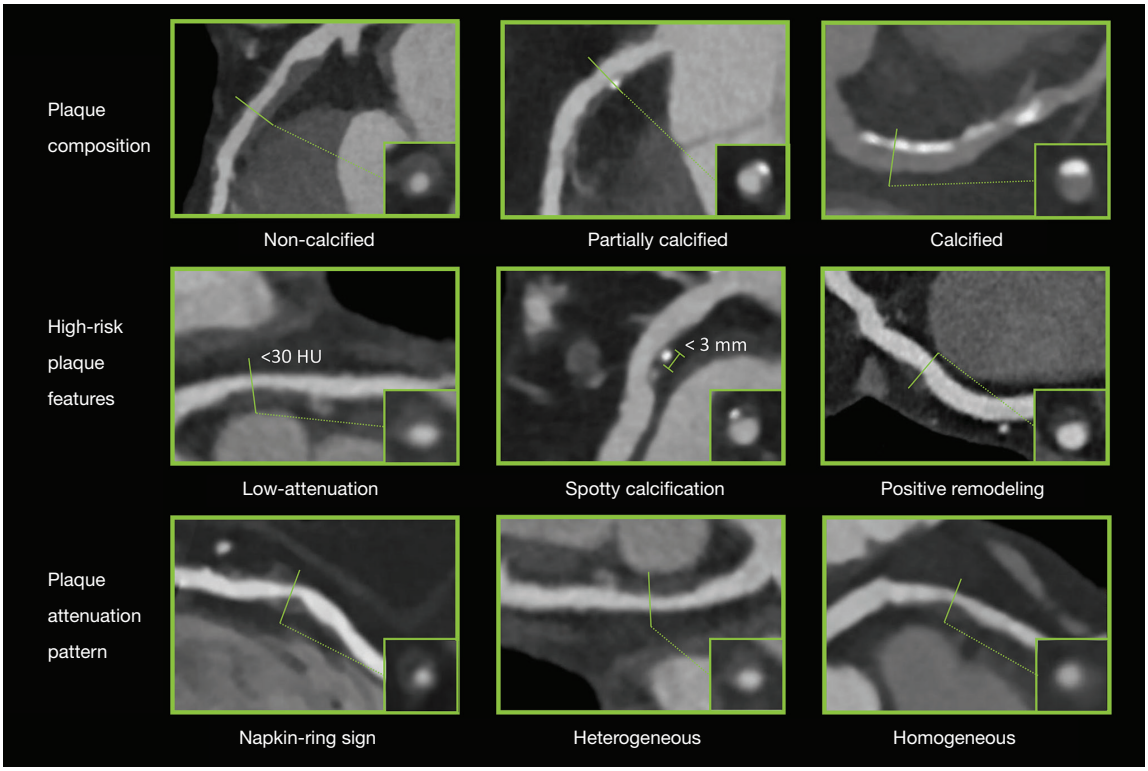

Figure 1 Representative images of plaque characteristics identifiable using coronary CT angiography (CTA).

a specific type of plaque as compared to patients without any plaques.

Overall, the effect of plaque composition on mortality still remains controversial. It seems simply classifying plaques based on the amount of calcium present holds little information regarding clinical outcome. These findings suggest, that identification of more complex morphologies are needed for better prediction of adverse outcomes.

Plaque attenuation and pattern

Histopathologic examinations demonstrated that thin-cap fibroatheromas (TCFA) exhibit similar plaque morphologies as ruptured plaques (20,27). TCFAs are composed of a lipid-rich necrotic core surrounded by a thin fibrotic cap. Coronary CTA is capable of distinguishing between lipid-rich and fibrotic tissue based on different CT attenuation values, however the reliable classification of non-calcified plaques into these two categories remains challenging.

Several studies have investigated the use of region of interest (ROI) to define the plaque components using coronary CTA as compared to intravascular ultrasound (IVUS) as the gold standard of *in vivo* plaque characterization (28-31). These validation studies were able to find significant differences in mean Hounsfield Unit (HU) values for the different plaque components, however there is a considerable overlap between these categories (121±34 *vs.* 58±43 HU, P<0.001) (28). Several studies were inspired by these results and investigated the mean and minimal attenuation values of plaques in ACS patients as compared to plaques of stable angina patients and found lower attenuation values for ACS patients (32-34). However, there was still a significant overlap in attenuation values between the two groups. Nevertheless, Motoyama *et al.* showed that with the use of a strict cut-off value (<30 HU), ACS patients have significantly more low attenuation plaques as compared to stable angina patients (79% *vs.* 9%, P<0.001), suggesting low attenuation to be a useful marker for identifying vulnerable patients (35). Marwan *et al.* proposed a more quantifiable approach using quantitative histogram analysis. For all cross-sections for each plaque, a histogram was created from the CT attenuation numbers, and the percentage of pixels with a density ≤30 HU was

calculated. They found similarly overlapping HU values for lipid-rich versus fibrous plaques. However, using a cut-off value of 5.5% for pixels with ≤30 HU, they were able to differentiate between predominantly lipid-rich plaques versus predominantly fibrous plaques (sensitivity: 95%; specificity: 80%; area under the curve: 0.9) using IVUS as reference standard (36). Despite these encouraging results, there is still a major concern because of the overlapping HU values of different plaque components. Furthermore, several studies have shown slice thickness (37), imaging protocols (38), tube voltage settings (39), intracoronary contrast attenuation values (40), reconstruction algorithms, filters and noise (37,41) all to influence CT attenuation values. Overall, it seems discrimination of non-calcified plaques based on HU value thresholds into lipid-rich and fibrous categories has additional prognostic value, but the different modifying effects of image acquisition and reconstruction limit the robust use of attenuation values for patient risk prediction.

Another more qualitative approach is not to look at the absolute HU values, but rather to classify non-calcified plaques as homogeneous or heterogeneous in attenuation patterns (*Figure 1*). Heterogeneous plaques are characterized by at least two regions with different attenuations values, while homogeneous plaques do not have regions visually differentiable. Based on cross sectional images, heterogeneous plaques can be divided into ones with napkin-ring sign (NRS) and ones without (42). NRS plaques are characterized by a low attenuation central area, which is apparently in touch with the lumen, encompassed by a higher attenuation ring-like peripheral area (43). Maurovich-Horvat *et al.* showed based on *ex vivo* examinations that NRS plaques have excellent specificity and low sensitivity (98.9%; 24.4%, respectively) to identify plaques with a large necrotic core, which is a key feature of rupture prone TCFA's (44). Histological evaluation of NRS plaques showed that NRS plaques had greater area of lipid-rich necrotic core (median 1.1 *vs.* 0.5 mm^2, P=0.05), larger non-core plaque area (median 10.2 *vs.* 6.4 mm^2, P<0.01) and larger vessel area (median 17.1 *vs.* 13.0 mm^2, P<0.01) as compared to non-NRS plaques (45). Interestingly, these results are in line with Virmani *et al.* who investigated the morphology of ruptured plaques (20). Furthermore, results of the Rule Out Myocardial Infarction/Ischemia Using Computer-Assisted Tomography-II (ROMICAT-II) trial strengthen the concept of NRS plaques being precursors of ruptured plaques. Based on the results of 472 patients suspected of ACS they found NRS plaques to be an independent predictor of ACS (odds ratio: 8.9; 95% CI: 1.8–43.3; P=0.006) independent of stenosis severity (46). Kashiwagi *et al.* found similar results, when analyzing the results of ACS patients and stable angina patients. They found NRS plaques to be more frequent at culprit and also at non-culprit sites in ACS patients as compared to stable angina patients (culprit: 49.0% *vs.* 11.2%, P<0.01, respectively; non-culprit: 12.7% *vs.* 2.8%, P<0.01, respectively) (47). Otsuka *et al.* conducted the first prospective clinical trial to assess the predictive values of NRS plaques for future ACS events (48). They showed that NRS plaques were significant independent predictors of later ACS events [hazard ratio: 5.55 (95% CI: 2.10–14.70)]; P<0.001. Similarly, a recently published study by Feuchtner *et al.* showed NRS to have the highest hazard ratio (7.0; 95% CI: 2.0–13.6) over other high risk features when investigating 1,469 patients with a mean follow-up of 7.8 years (49).

Overall it seems both plaque attenuation and pattern have additive information beyond simple plaque composition information. However, with many factors effecting assessment of attenuation values and patterns, we only have limited censored information regarding the prognostic effect of these entities.

Spotty calcification

Histological examinations identified calcified nodules in patients with coronary thrombosis (50). Several histological studies have shown the frequency of such findings to be around 2–7% in sudden death cases (51-53). Intra-plaque microcalcifications are thought to destabilize plaques and promote plaque rupture (54,55). Unfortunately, spatial resolution of current CT scanners is under the threshold needed for identifying microcalcification. Nevertheless, coronary CTA has excellent sensitivity to identify calcium, thus spotty calcification defined as a <3 mm calcified plaque component with a >130 HU density surrounded by non-calcified plaque tissue has been proposed as a CTA marker of histological microcalcifications (35,56) (*Figure 1*). van Velzen *et al.* suggested to further classify such lesions as small (<1 mm), intermediate (1–3 mm), and large (>3 mm) (57). They found small spotty calcifications to be more frequently present with TCFA's identified by IVUS as compared to large spotty calcifications (31% *vs.* 9%; P<0.05). These results support the hypothesis, that small calcified nodules are indicators of high-risk plaques, and that CTA is at the limits of identifying real calcified nodules, which have been identified using histological

studies. Even so, several studies have shown culprit lesions of ACS patients to have spotty calcifications as compared to stabile angina patients or non-culprit lesions (32,34,35,58). However, there are only few prospective studies evaluating the prognostic effect of spotty calcifications, thus the relationship between intra-plaque calcification and future cardiac events remains uncertain (59).

A promising technique for the identification of microcalcifications beyond the resolution limits of CTA is PET imaging (60). Dweck *et al.* used 18F-sodium fluoride to mark microcalcifications not visible on CTA. 18F-sodium fluoride has been used previously for decades to image new bone formation, primarily cancer metastases, and recently has been used to image active calcification in coronary plaques. In their study based on 119 volunteers, they showed higher uptake values in patients with prior cardiovascular events, angina and higher Framingham risk scores, as compared to control subjects (P=0.016; P=0.023; P=0.011, respectively).

Altogether, it seems spotty calcifications have additional additive values for identifying vulnerable plaques. However current resolution of CT scanners prohibits the imaging of microcalcifications that are seen as one of the common features of ruptured plaques. Nevertheless, spotty calcification detectable using CTA seems to correlate well with adverse cardiac events, and 18F-sodium fluoride PET is also a promising new technique to visualize microcalcifications. However prospective studies are needed to evaluate the predictive value of these markers.

Positive remodeling

Atherosclerotic plaques initially tend to grow outwards leaving luminal integrity unchanged (61). Thus while many coronary plaques accumulate lipids and become TCFAs, they might not cause any clinical symptoms. This phenomenon is referred to as positive remodeling (*Figure 1*). Varnava *et al.* examined 88 sudden cardiac death cases and showed that plaques with positive remodeling have larger lipid cores and more macrophages, both which are considered vulnerability markers (62). Using coronary CTA, the remodeling index is calculated as the vessel cross-sectional area at the level of the maximal stenosis divided by the average of the proximal and distal reference sites' cross-sectional areas (63). Coronary CTA has a tendency to overestimate remodeling index, thus Gauss *et al.* proposed a cut-off value of ≥1.1, meaning a 10% increase in the vessel cross sectional area at the site of the maximal stenosis compared to the average of the reference cross sectional areas (64). This resulted in an increased sensitivity and a moderate drop in specificity as compared to a lower cut-off value of ≥1.05 (sensitivity: 78% *vs.* 45%; specificity: 78% *vs.* 100%) using IVUS as reference standard. Motoyama *et al.* showed positively remodeled plaques to be more frequent in ACS patients as compared to stable angina patients (87% *vs.* 12%, P<0.0001, respectively) (35). Positive remodeling had the best sensitivity and specificity (87%; 88%, respectively) as compared to low-attenuation and spotty calcification to identify ACS patients (65).

Overall it seems that positive remodeling is an important plaque feature for the identification of vulnerable plaques. Being less conditional to image noise as plaque attenuation, and having a more quantitative definition as the NRS, positive remodeling might become a more robust marker for vulnerable plaques. However, more prospective studies are needed to assess the effect of positive remodeling on later outcomes.

Altogether we can say that distinct plaque morphologies can be identified using coronary CTA which are associated with adverse cardiac events. However, many question the concept of the vulnerable plaque (66,67). Kubo *et al.* showed that 75% of TCFA's lost their vulnerability characteristics after 1 year, while only 25% remained to be classified as TCFA using IVUS (68). Furthermore, the Providing Regional Observations to Study Predictors of Events in the Coronary Tree (PROSPECT) study demonstrated that the maximum annualized risk of myocardial infarction or cardiovascular death is only 0.06% per year for a single vulnerable plaque, which is much smaller risk than what is conventionally considered high risk (69,70). These results indicate that even though coronary CTA is capable of identifying vulnerable markers which correlate with gold-standard histological findings, these characteristics currently are not able to explain all aspects of later outcomes and thus we must also consider stenosis severity and overall CAD burden.

Stenosis assessment with coronary CTA

Based on guidelines published by the Society of Cardiovascular Computed Tomography (SCCT), luminal stenosis can be graded as: minimal (<25% stenosis), mild (25% to 49% stenosis), moderate (50% to 69% stenosis), severe (70% to 99% stenosis) and occluded (71) (*Figure 2*). As coronary plaques grow, blood flow is eventually disrupted causing ischemia distal to the lesion. Originally coronary CTA was considered as a non-invasive alternative

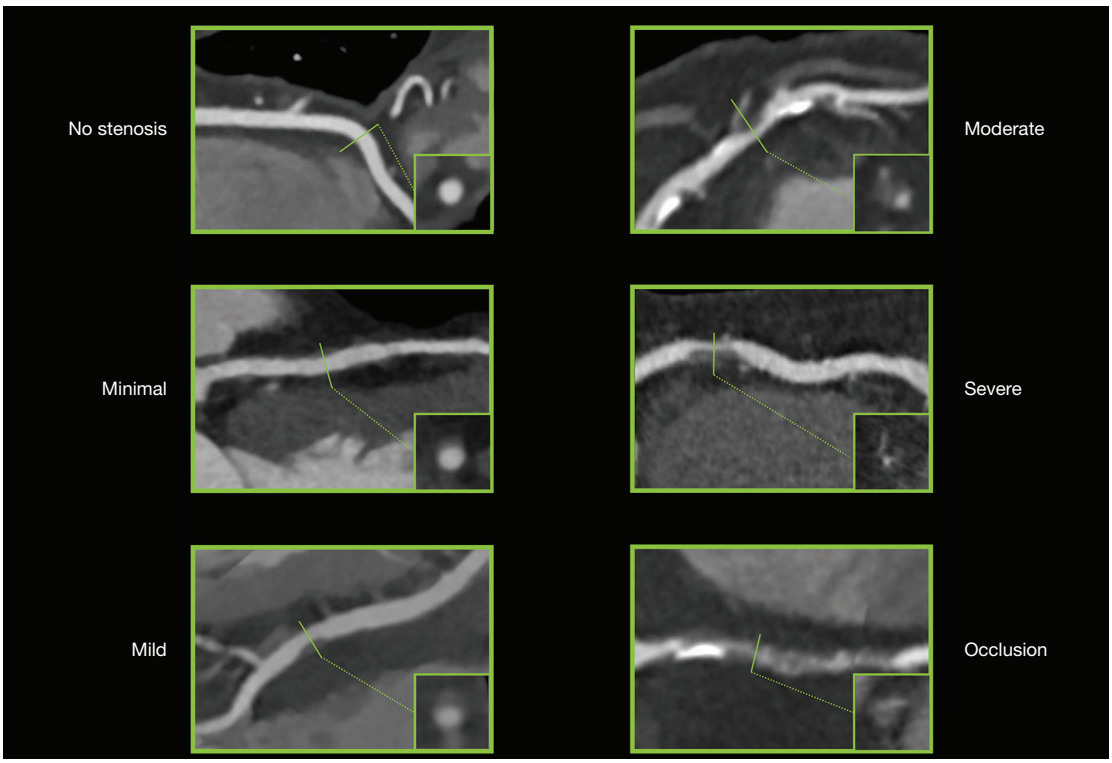

Figure 2 Representative images of stenosis categories using coronary CT angiography (CTA).

to ICA, thus many studies have looked into the predictive value of luminal stenosis seen on CTA. All studies focus on obstructive lesions, since most patients referred to coronary CTA have minimal and mild plaques, thus the predictive value of such stenosis is poor. Two cut-off values: ≥50% and ≥70% diameter stenosis are frequently used to determine obstructive lesions. Min *et al.* investigated the prognostic effect of obstructive lesion on a patient-based level and found both ≥50% and ≥70% lesions to be significant predictors of later outcomes (hazard ratio: 2.89; 4.31, respectively) (72). Several other studies have also found obstructive lesions to be significant predictors of later outcome, but considerably different hazard ratios have been reported (24,73-77). Interestingly, there is a discrepancy in the results when correcting the models for clinical risk factors. The significant hazard ratios reported by Min *et al.* became non-significant when including cardiac risk factors in the model, but when looking at a segment-based level not a patient based level, the presence of obstructive stenosis remained significant, but with a smaller hazard ratio (1.05; 95% CI: 1.02–1.09) (72). However, Nakazato *et al.* and Andreini *et al.* did not find similar tendencies when correcting for clinical factors, as obstructive CAD remained a significant predictor (74,76). Increasing further the discrepancy in the results, a 5-year follow-up study published by Hadamitzky *et al.* reported that while non-obstructive CAD was a significant predictor of hard endpoints (hazard ratio: 3.33; 95% CI: 1.40–7.91), one and two vessel obstructive disease was not (hazard ratio: 1.46; 95% CI: 0.50–2.43; 3.85; 95% CI: 0.96–15.04) (24).

One explanation for the disparity in the results might be that luminal stenosis on CTA is a poor indicator of hemodynamically significant lesions (78), which has been shown to be a good predictor of adverse events (79-81). Using computational fluid dynamics it is possible to simulate blood flow in the coronaries and estimate the hemodynamic characteristics of a lesion with good diagnostic accuracy (82,83). The Prospective LongitudinAl Trial of FFRct: Outcome and Resource IMpacts (PLATFORM) study further demonstrated, that the use of CT derived fractional flow reserve (FFR-CT) values significantly lowered the rate of ICA and used less resources at lower costs (84-86). However, current FFR-CT simulations are expensive and time consuming, as the simulations are performed off-site. Recently on-site FFR-CT techniques have been introduced, which are able to calculate FFR-CT in a couple of seconds

to minutes (87-90). Further studies are warranted to explore the diagnostic accuracy and utility of these novel on-site algorithms. As an alternative to FFR-CT transluminal attenuation gradient (TAG) measurement was proposed, which tries to estimate hemodynamic significance by calculating the drop in HU values proximal and distal to the lesion (91,92). Unfortunately, validation studies comparing TAG to invasive FFR values showed poor accuracy results (sensitivity: 58%; specificity: 86%; positive predictive value: 64% negative predictive value 83%) (93), with area under the curve values equal to the flip of a dime (AUC =0.50) (94). A more qualitative method is the area of stenosis, lesion length, and APPROACH (ASLA) score (95), which uses plaque burden, minimal luminal area and diameter, stenosis diameter, area of stenosis, lesion length, remodeling index, plaque morphology, calcification severity, and the Alberta Provincial Project for Outcome Assessment in Coronary Heart Disease (APPROACH) score (96), which estimates the amount of myocardium at risk to identify hemodynamically significant lesions. Based on 85 patients, Ko *et al.* demonstrated that the ALSA score was superior to area stenosis, lesion length and the APPROACH score in predicting significant FFR values (95). Another approach to evaluate hemodynamic relevance of coronary lesions is CT myocardial perfusion (97). CTA therefore could provide comprehensive assessment of CAD incorporating both morphological and functional information to accurately detect significant coronary stenosis. Yang *et al.* evaluated 72 patients with rest CT perfusion imaging, on-site CT-FFR and invasive FFR (90). Combination of anatomical assessment with on-site CT-FFR or CT perfusion imaging significantly improved diagnostic accuracy (0.86 *vs.* 0.92, P=0.004; 0.86 *vs.* 0.91, P=0.004, respectively).

All in all, it seems the effect of significant stenosis on patient outcomes is controversial, which is mainly caused by the poor correlation between stenosis seen on CTA and hemodynamic information. Furthermore, several studies have shown that the more vessels are involved the higher the hazard ratio. This shows the need not only to look at single plaque features or stenosis, but to also look at the extent of CAD.

Plaque burden assessment with coronary CTA

Several studies, such as the Clinical Outcomes Utilizing Revascularization and Aggressive Drug Evaluation (COURAGE) trial showed that plaque burden assessment may be more important than ischemic myocardium burden for predicting later major adverse outcomes (98). Furthermore, Bittencourt *et al.* demonstrated that patients with extensive CAD (> four segments involved) have similar hazard ratios for developing major adverse outcomes as compared to patients with obstructive disease with less than five segments involved, thus also emphasizing the importance of quantifying plaque burden (14). Min *et al.* proposed a score system, the segment stenosis score (SSS) and the segment involvement score (SIS) to quantify plaque burden (72). SSS is calculated by grading all coronary segments as: 0, no plaque; 1, <50% stenosis; 2, 50–69% stenosis; 3, ≥70% stenosis. SIS is the number of affected segments. Based on 1,127 patients, SSS had a hazard ratio of 1.99 (95% CI: 1.48–2.67), while SIS had a hazard ratio of 1.23 (95% CI: 1.13–1.34). Similarly, results from the CONFIRM registry also showed SIS to be an independent predictor of later major adverse events (hazard ratio: 1.22; 95% CI: 1.03–1.44) (15). Several other studies have also demonstrated SSS and SIS to be significant independent predictors of later outcomes (24,74,99,100). While SSS and SIS are simple and elegant concepts for describing plaque burden, they are conceptually flawed. SSS and SIS scores assume that plaque burden is additive, meaning that adding one plaque to already two diseased segments or 12 diseased segments has the same effect. Furthermore, SSS and SIS lose all anatomical information, thus they assume a moderate stenosis on the left main has the same effect as a moderate stenosis on the second diagonal branch, which clearly is not true. Results of the CONFIRM trial also emphasize the importance of lesion characteristics and location. They found that excluding distal segments and only considering the number of proximal segments with obstructive plaques significantly improved their prediction model (15). Another approach for quantifying the magnitude of plaque burden is the 3-vessel score, which counts how many major epicardial vessels (left anterior descending, left circumflex, right coronary) have obstructive stenosis (72). Andreini *et al.* demonstrated that having only one major epicardial vessel effected with an obstructive lesion (≥50%) has a hazard ratio of 3.18 (95% CI: 2.16–4.69), if all three vessels are effected, the hazard ratio increases to 7.10 (95% CI: 4.61–10.93) (74). Similar tendencies have been reported by several studies (24,72,99-102). A more quantitative approach originally developed to characterize CAD severity using ICA (103), later adopted for coronary CTA is the Duke CAD Index (72,104). Patients are assigned a risk score between 0–100 based on former patient prognosis data (103). The score is an

Table 1 Modified Duke Coronary Artery Disease Index for coronary CTA

Extent of coronary artery disease	Points
Stenosis <50%	0
Stenosis ≥50%	
1 vessel	23
2 vessel	37
3 vessel	56
Stenosis ≥50% and proximal LAD stenosis ≥50%	
1 vessel	48
2 vessel	56
3 vessel	74
Left main stenosis	
≥50%	80
≥70%	100

Score system is based on Miller *et al.* In the Modified Duke Coronary Artery Disease Index patients are assigned to the most severe category. CTA, CT angiography; LAD, left anterior descending.

extension of the 3-vessel disease score. It also incorporates stenosis severity and calculates with left main stenosis and proximal left anterior descending stenosis (*Table 1*). Min *et al.* showed that there was a significant difference between patients' cumulative survival for the different categories (72). Left main plaque with any additional moderate or severe stenosis had the worst outcome, while patients without any disease or only mild CAD had almost no events.

Altogether, plaque burden assessment seems to be a very important concept to describe the severity of CAD and predict adverse outcome. Several methods have been proposed to properly quantify plaque burden, indicating the lack of a single best method. Furthermore, as we have seen, not only plaque burden, but plaque localization, stenosis severity, plaque composition and vulnerability features all play a role in later outcomes, thus necessitating a more complex holistic approach, which incorporates as many of these parameters as possible (43).

Composite plaque burden score assessment with coronary CTA

Based on research investigating the risk of plaque features and extension of CAD, several attempts have been made to create composite scores incorporating anthropometric vulnerability with extent of CAD, plaque localization and vulnerability features as assessed by CTA.

CONFIRM risk score

The CONFIRM registry is an international prospective observational cohort currently with seven participating countries (22). Structured interviews were used to collect information regarding patients' anthropometrics and cardiovascular risk profile. Using this information the National Cholesterol Education Program Expert Panel on Detection, Evaluation, and Treatment of High Blood Cholesterol in Adults (NCEP ATP III) (105), the Framingham (106) and the Morise clinical risk scores were calculated (23). The 16-segment coronary artery model was used to assess the CTA images (107). Each coronary segment was evaluated for the presence of plaque. Plaques were classified as calcified, partially calcified or non-calcified. The degree of stenosis was graded as: none (0% luminal stenosis); mild (1% to 49% luminal stenosis); moderate (50% to 69% luminal stenosis); or severe (≥70% luminal stenosis).

Overall, 17,793 patients' data was used to create the CONFRIM risk score using multivariate Cox proportional hazard models (15). The resulting models were evaluated using a separate test set, which consisted of 2,506 patients' data. After separate assessment of clinical risk scores and CTA imaging markers, a combined score was created. The COMFIRM risk score is a combination of the NCEP ATP III score, the number of proximal segments [proximal and mid right coronary artery (RCA), left main, proximal, and mid left anterior descendent, proximal circumflex, first obtuse marginal branch] with stenosis greater than 50%, and the number of proximal segments with partially calcified or calcified plaques. Adding these two additional parameters caused 32% of the patients to be reclassified, 22% to a lower risk category and 10% to a higher category. Overall, the combined risk score outperformed all clinical scores and significantly improved prediction of all-cause mortality. A online calculator is available for the CONFIRM risk score (108).

Leaman score

Originally the Leaman score was established based on ICA measurements. Since plaque features cannot be visualized

Table 2 CTA adapted Leaman score weighing factors

Segments	Dominance		
	Right dominance	Left dominance	Balanced
Proximal RCA	1.0	0	0.5
Mid RCA	1.0	0	0.5
Distal RCA	1.0	0	0.5
R-PDA	1.0	–	0.5
R-PLB	0.5	–	–
Left main	5.0	6.0	5.5
Proximal LAD	3.5	3.5	3.5
Mid LAD	2.5	2.5	2.5
Distal LAD	1.0	1.0	1.0
1st diagonal	1.0	1.0	1.0
2nd diagonal	0.5	0.5	0.5
IM	1.0	1.0	1.0
Proximal LCX	1.5	2.5	2.0
1st OM	1.0	1.0	1.0
Mid-distal LCX	0.5	1.5	1.0
2nd OM	1.0	1.0	1.0
L-PDA	–	1.0	–
L-PLB	–	0.5	0.5
Stenosis severity			
Obstructive	1.000	–	–
Non-obstructive	0.615	–	–
Plaque composition			
Non-calcified or partially calcified	1.5	–	–
Calcified	1	–	–

CTA adapted Leaman-score is calculated by multiplying the weighing factors regarding plaque composition, stenosis severity and location for a given segment. Overall score is calculated by summing up scores for all segments. RCA, right coronary artery; R-PDA, posterior descending artery originating from right coronary; R-PLB, posterolateral branch originating from right coronary; LAD, left anterior descending; IM, intermediate branch; LCx, left circumflex; OM, obtuse marginal; L-PDA, posterior descending artery originating from left coronary; L-PLB, posterolateral branch originating from left coronary.

using ICA, only the localization and the degree of stenosis is used to calculate the score. Obstructions are weighted based on typical amount of blood flow to the left ventricle going through that given segment. On average in case of right dominant coronary anatomy, the RCA receives 16%, while the left main trunk delivers 84% of the blood flow going the left ventricle (109). For left dominant coronary systems, all of the left ventricle is supplied by the left coronary artery. Weighting factors are equal to how many times more blood goes through a given segment as compared to the RCA. For left dominant systems, the RCA receives a weighting factor of zero, while the weighting factor of the LM and circumferential segments increases by one (110). The degree of stenosis was also accounted for. Occlusions receive a multiplication factor of five, 90–99% stenosis receive multiplication factor of three and obstructions between 70–89% receive a multiplication factor of one. Non-obstructive lesion (<70%) are not accounted for. A patients' Leaman score is equal to the sum of all segment scores for all 16 segments (107).

CTA adapted Leaman score as proposed by de Araújo Gonçalves *et al.* (111) has minor modifications as compared to the original publication of Leaman *et al.* (110). To account of balanced coronary systems an intermediate value was used for segments where there was a difference in the weighting factors for left and right dominant systems. Plaque composition was also included. For non-calcified and partially calcified plaques weighting factor of 1.5 is added, while calcified plaques receive a weighting factor of one. Lesions with <50% stenosis receive a multiplication factor of 0.615 which is the relative proportion of the hazard ratios for mortality between obstructive and non-obstructive CAD, as reported by Chow *et al.* from the CONFIRM registry (112). A summary of the calculation can be found in *Table 2*.

Mushtaq *et al.* evaluated the CTA adapted Leaman score using a single-center prospective registry including 1,304 consecutive patients (113). Hard cardiac events (cardiac death and nonfatal myocardial infarction) were considered primary end-points. Using multivariate Cox regression models which included clinical parameters and SSS or SIS or the CTA adapted Leaman score, were all independent predictors of adverse events. The Leaman score had the highest hazard ratio as compared to the other two scores (hazard ratio: Leaman score: 5.39, 95% CI:

3.49–8.33; SSS: 4.42, 95% CI: 2.97–6.57; SIS: 3.09, 95% CI: 2.00–4.75, respectively). The event free survival of patients with Leaman scores in the highest tercile (score >5) and obstructive CAD was similar to patients with similar Leaman scores but without obstructive CAD (78.6% *vs.* 76.5%; P=0.627).

SYNTAX score

Originally the SYNergy between percutaneous coronary intervention with TAXus and cardiac surgery (SYNTAX) score was developed to quantify the complexity of CAD, and to determine optimal revascularization strategies for multi-vessel CAD patients (114). SYNTAX score incorporates multiple score systems. As opposed to previously described CTA scores, the SYNTAX score is a lesion based scoring system, rather than a segment based system, thus multiple lesions can be present and also scored in the same segment.

The original 16-segment classification of the American Heart Association (107) is extended based on the arterial revascularization therapies study (115), to include additional side branches. Only vessels greater than 1.5 mm and lesions with a stenosis greater than >50% are analyzed. The SYNTAX score does not recognize balanced coronary dominance. Each lesion receives the Leaman score values for the segments in which it is present (*Table 2*). Each segment score is multiplied by two for non-occlusive lesions (50–99%) and by five for occlusive lesions (100%). Only one segment is allowed to be occlusive for each lesion. Additional lesion attributes are scored based on the ACC/AHA lesion classification system (116). Characteristics of occlusions (117), involvement of trifurcations, bifurcations (118,119) and aortal ostium, severe tortuosity, lesion length, heavy calcification, thrombus and diffuse coronary disease are all accounted for. Further adverse lesion characteristics are all additive. Details of the scoring system are described in *Table 3*.

The SYNTAX score includes many vulnerability parameters, thus utilization of the scoring system for long-term prognosis seems rational. Suh *et al.* evaluated the performance of the SYNTAX score based on 339 patients who underwent both CTA and ICA (120). Only characteristics assessable by both CTA and ICA were included in the SYNTAX score. Based on univariate Cox regression analysis age, 3-vessel or LM disease on CCTA, 2-vessel disease or 3-vessel or LM disease on ICA, and SYNTAX scores higher than 23 based on ICA were predictors of MACE. On the contrary, multivariate analysis showed that models incorporating the SYNTAX score or simply the number of involved vessels had similar predictive power, both in case of CTA (area under the curve: 0.701 *vs.* 0.659, respectively) and ICA (area under the curve: 0.706 *vs.* 0.676, respectively). Recently, the SYNTAX score II has been developed that combines the SYNTAX score

Table 3 Scoring system of the SYNTAX score

Characteristics	Points
Stenosis	
Occlusion	×5
Significant lesion	×2
Aorto ostial stenosis	+1
Occlusion characteristics	
Age >3 months or unknown	+1
Blunt stump	+1
Bridging	+1
First segment visible beyond occlusion	+1 per non-visible segment
Side branch	+1
Trifurcations	
1 diseased segment	+3
2 diseased segments	+4
3 diseased segments	+5
4 diseased segments	+6
Bifurcations	
Type A, B, C	+1
Type D, E, F, G	+2
Angulation <70°	+1
Severe tortuosity	+2
Lesion length >20 mm	+1
Heavy calcification	+2
Thrombus	+1
Diffuse disease of affected vessel	+1 per number of segments

SYNTAX score is calculated by multiplying the Leaman score (*Table 2*) of the segments which contain the given lesion by the stenosis factor. Further lesion characteristics are all additive. Overall, the SYNTAX score is the sum of all individual lesion scores. +, addition; ×, multiplication.

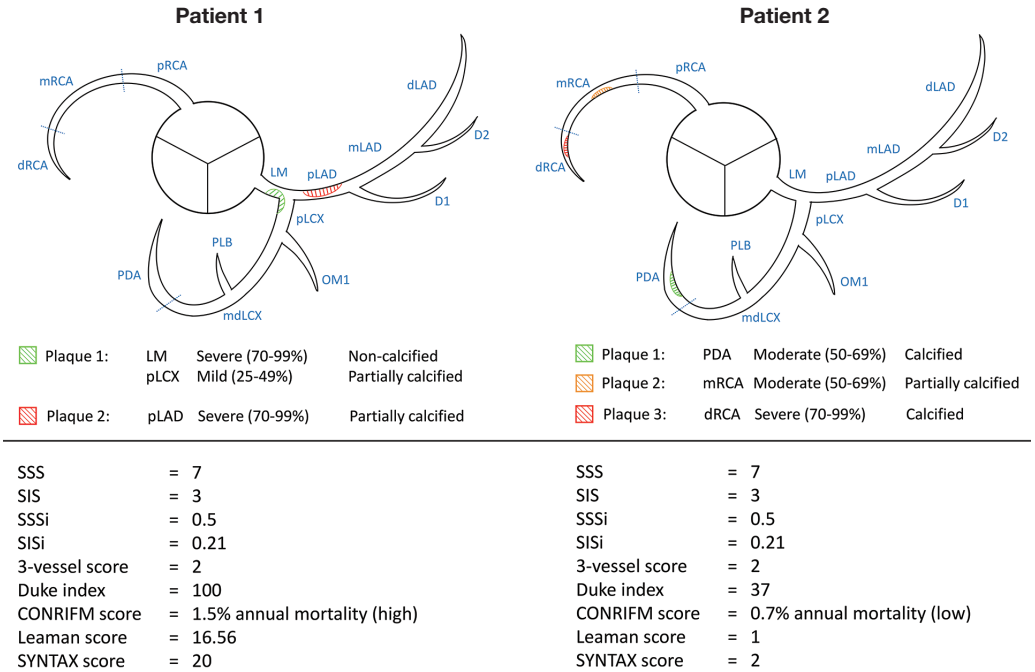

Figure 3 Representative examples of plaque burdens and composite plaque scores. For the CONFIRM score both patients were assumed to be 65-year-old smoking male patients with 230 mg/dL total cholesterol, 47 mg/dL HDL, 142 mmHg systolic blood pressure using hypertension medication. For the SYNTAX score calculations, the LAD-LCX bifurcation was assumed to be ≥70° and all plaques were shorter than 20 mm. The example shows, that patients with very different degree of disease can have very similar plaque burden scores. Composite plaque burden scores on the other hand seem to better differentiate between the severity of coronary artery disease. D, diagonal; IM, intermediate branch; LAD, left anterior descending; LCX, left circumflex; PDA, posterior descending artery; PLB, posterolateral branch; OM, obtuse marginal; RCA, right coronary artery; prefixes: d, distal; m, mid; p, proximal.

with clinical variables (121). Long-term follow-up data are promising based on ICA, but we currently lack CTA-based results. Based on these results, it seems incorporating an exceedingly complex score system, such as the SYNTAX score, is not justifiable, since it has no proven additive value in risk prediction, as compared to simple CTA based CAD burden scores.

Overall, composite plaque burden scores seem to be a valid concept to determine the severity of CAD. One major flaw of simple plaque burden scores is that very different disease severities can have very similar scores (*Figure 3*). Composite scores seem to account for this, but one must not forget, that these scores are only useful if they are calculated. The calculation of composite scores can become very complex, adding an additional burden to the clinicians. In the future, with the use of structured reporting platforms, these values can be calculated and evaluated automatically by the program. Therefore, these scores could transition from simple research interests to clinically useful risk stratification systems.

Disadvantages of coronary CTA

Even though coronary CTA is a non-invasive technique, there are still some risks one has to consider. CT uses radiation for image acquisition, thus there is an increased risk for radiation induced illnesses, such as cancer (122). Some estimates show that up to 1.5% to 2.0% of all cancers can be associated to CT use (123). Furthermore, to achieve proper image quality high intraluminal contrast media concentrations need to be reached. However, high contrast volumes and high injection rate increases the risk of contrast induced nephropathy and contrast media extravasation (124,125). In addition, coronary CTA provides detailed information regarding coronary plaques, but only provides limited information regarding the functional significance of CAD. New techniques such as CT myocardial perfusion can add valuable information regarding myocardial ischemic

burden, but improvement of diagnostic performance is achieved through additional radiation exposure (90,97).

Future directions

Quantitative plaque assessment

Radiological images can not only be visually inspected, but can also be looked at as vast three-dimensional datasets. Using coronary segmentation software, one can delineate the lumen and the vessel wall to receive volumetric information regarding the composition of the coronary wall. One major concern is the fact that HU values are effected by several different factors (37-41), thus precise classification of plaque components is difficult. Nevertheless, there are encouraging results indicating that quantitative plaque assessment might hold additional information for predicting later outcomes (126-129).

Radiomics

Radiomics is the process of extracting quantitative features for radiological images and converting them into minable datasets, which can be further analyzed using data mining and machine learning algorithms (130,131). Radiomics also integrates clinical and genetic information to make a comprehensive multi-dimensional database, which can be used not only for population based statistical inference, but also for individual patient based risk assessment. This holistic approach has shown promising results in oncology imaging (132,133), but utilization to cardiovascular imaging is scarce.

Conclusions

Coronary CTA has evolved like no other non-invasive imaging modality over the past decade. A couple of years ago only considered as a "gate-keeper" for ICA, is now thought of as versatile imaging modality capable of depicting atherosclerosis *in vivo*. With the advances of image quality, so did our understanding regarding the different aspects of CAD. All the results indicate that coronary CTA is a valuable tool for predicting patient outcomes. However, a more holistic approach is needed, accounting for many different features of atherosclerosis. For this, new characteristics need to be defined and new statistical methods need to be employed. However strenuous this may be, the reward is not less than decreasing the burden of cardiovascular morbidity and mortality on a global scale.

Acknowledgements

Funding: The study was supported by the National Research, Development and Innovation Office of Hungary (NKFIA; NVKP-16-1-2016-0017).

Footnote

Conflicts of Interest: The authors have no conflicts of interest to declare.

References

1. Schwartz RB, Jones KM, Chernoff DM, et al. Common carotid artery bifurcation: evaluation with spiral CT. Work in progress. Radiology 1992;185:513-9.
2. Napel S, Marks MP, Rubin GD, et al. CT angiography with spiral CT and maximum intensity projection. Radiology 1992;185:607-10.
3. Rubin GD, Shiau MC, Schmidt AJ, et al. Computed tomographic angiography: historical perspective and new state-of-the-art using multi detector-row helical computed tomography. J Comput Assist Tomogr 1999;23 Suppl 1:S83-90.
4. Rubin GD, Shiau MC, Leung AN, et al. Aorta and iliac arteries: single versus multiple detector-row helical CT angiography. Radiology 2000;215:670-6.
5. Achenbach S, Ulzheimer S, Baum U, et al. Noninvasive coronary angiography by retrospectively ECG-gated multislice spiral CT. Circulation 2000;102:2823-8.
6. Hu XH, Zheng WL, Wang D, et al. Accuracy of high-pitch prospectively ECG-triggering CT coronary angiography for assessment of stenosis in 103 patients: comparison with invasive coronary angiography. Clin Radiol 2012;67:1083-8.
7. Budoff MJ, Dowe D, Jollis JG, et al. Diagnostic performance of 64-multidetector row coronary computed tomographic angiography for evaluation of coronary artery stenosis in individuals without known coronary artery disease: results from the prospective multicenter ACCURACY (Assessment by Coronary Computed Tomographic Angiography of Individuals Undergoing Invasive Coronary Angiography) trial. J Am Coll Cardiol 2008;52:1724-32.
8. de Graaf FR, van Velzen JE, de Boer SM, et al. Non-

invasive computed tomography coronary angiography as a gatekeeper for invasive coronary angiography. Int J Cardiovasc Imaging 2013;29:221-8.
9. Shaw LJ, Hausleiter J, Achenbach S, et al. Coronary computed tomographic angiography as a gatekeeper to invasive diagnostic and surgical procedures: results from the multicenter CONFIRM (Coronary CT Angiography Evaluation for Clinical Outcomes: an International Multicenter) registry. J Am Coll Cardiol 2012;60:2103-14.
10. Virmani R, Kolodgie FD, Burke AP, et al. Lessons from sudden coronary death: a comprehensive morphological classification scheme for atherosclerotic lesions. Arterioscler Thromb Vasc Biol 2000;20:1262-75.
11. Ambrose JA, Tannenbaum MA, Alexopoulos D, et al. Angiographic progression of coronary artery disease and the development of myocardial infarction. J Am Coll Cardiol 1988;12:56-62.
12. Glaser R, Selzer F, Faxon DP, et al. Clinical progression of incidental, asymptomatic lesions discovered during culprit vessel coronary intervention. Circulation 2005;111:143-9.
13. Farb A, Burke AP, Tang AL, et al. Coronary plaque erosion without rupture into a lipid core. A frequent cause of coronary thrombosis in sudden coronary death. Circulation 1996;93:1354-63.
14. Bittencourt MS, Hulten E, Ghoshhajra B, et al. Prognostic value of nonobstructive and obstructive coronary artery disease detected by coronary computed tomography angiography to identify cardiovascular events. Circ Cardiovasc Imaging 2014;7:282-91.
15. Hadamitzky M, Achenbach S, Al-Mallah M, et al. Optimized prognostic score for coronary computed tomographic angiography: results from the CONFIRM registry (COronary CT Angiography EvaluatioN For Clinical Outcomes: An InteRnational Multicenter Registry). J Am Coll Cardiol 2013;62:468-76.
16. Kolossváry M, Szilveszter B, Édes IF, et al. Comparison of Quantity of Coronary Atherosclerotic Plaques Detected by Computed Tomography Versus Angiography. Am J Cardiol 2016;117:1863-7.
17. Butler J, Shapiro M, Reiber J, et al. Extent and distribution of coronary artery disease: a comparative study of invasive versus noninvasive angiography with computed angiography. Am Heart J 2007;153:378-84.
18. Lusis AJ. Atherosclerosis. Nature 2000;407:233-41.
19. Stary HC, Chandler AB, Dinsmore RE, et al. A definition of advanced types of atherosclerotic lesions and a histological classification of atherosclerosis. A report from the Committee on Vascular Lesions of the Council on Arteriosclerosis, American Heart Association. Circulation 1995;92:1355-74.
20. Virmani R, Burke AP, Farb A, et al. Pathology of the vulnerable plaque. J Am Coll Cardiol 2006;47:C13-8.
21. Raff GL, Abidov A, Achenbach S, et al. SCCT guidelines for the interpretation and reporting of coronary computed tomographic angiography. J Cardiovasc Comput Tomogr 2009;3:122-36.
22. Min JK, Dunning A, Lin FY, et al. Rationale and design of the CONFIRM (COronary CT Angiography EvaluatioN For Clinical Outcomes: An InteRnational Multicenter) Registry. J Cardiovasc Comput Tomogr 2011;5:84-92.
23. Morise AP, Jalisi F. Evaluation of pretest and exercise test scores to assess all-cause mortality in unselected patients presenting for exercise testing with symptoms of suspected coronary artery disease. J Am Coll Cardiol 2003;42:842-50.
24. Hadamitzky M, Taubert S, Deseive S, et al. Prognostic value of coronary computed tomography angiography during 5 years of follow-up in patients with suspected coronary artery disease. Eur Heart J 2013;34:3277-85.
25. Dedic A, Kurata A, Lubbers M, et al. Prognostic implications of non-culprit plaques in acute coronary syndrome: non-invasive assessment with coronary CT angiography. Eur Heart J Cardiovasc Imaging 2014;15:1231-7.
26. Nance JW Jr, Schlett CL, Schoepf UJ, et al. Incremental prognostic value of different components of coronary atherosclerotic plaque at cardiac CT angiography beyond coronary calcification in patients with acute chest pain. Radiology 2012;264:679-90.
27. Virmani R, Burke AP, Kolodgie FD, et al. Pathology of the thin-cap fibroatheroma: a type of vulnerable plaque. J Interv Cardiol 2003;16:267-72.
28. Pohle K, Achenbach S, Macneill B, et al. Characterization of non-calcified coronary atherosclerotic plaque by multi-detector row CT: comparison to IVUS. Atherosclerosis 2007;190:174-80.
29. Voros S, Rinehart S, Qian Z, et al. Prospective validation of standardized, 3-dimensional, quantitative coronary computed tomographic plaque measurements using radiofrequency backscatter intravascular ultrasound as reference standard in intermediate coronary arterial lesions: results from the ATLANTA (assessment of tissue characteristics, lesion morphology, and hemodynamics by angiography with fractional flow reserve, intravascular ultrasound and virtual histology, and noninvasive computed tomography in atherosclerotic plaques) I study.

JACC Cardiovasc Interv 2011;4:198-208.
30. Leber AW, Becker A, Knez A, et al. Accuracy of 64-slice computed tomography to classify and quantify plaque volumes in the proximal coronary system: a comparative study using intravascular ultrasound. J Am Coll Cardiol 2006;47:672-7.
31. Sun J, Zhang Z, Lu B, et al. Identification and quantification of coronary atherosclerotic plaques: a comparison of 64-MDCT and intravascular ultrasound. AJR Am J Roentgenol 2008;190:748-54.
32. Pflederer T, Marwan M, Schepis T, et al. Characterization of culprit lesions in acute coronary syndromes using coronary dual-source CT angiography. Atherosclerosis 2010;211:437-44.
33. Yang X, Gai L, Dong W, et al. Characterization of culprit lesions in acute coronary syndromes compared with stable angina pectoris by dual-source computed tomography. Int J Cardiovasc Imaging 2013;29:945-53.
34. Kitagawa T, Yamamoto H, Horiguchi J, et al. Characterization of noncalcified coronary plaques and identification of culprit lesions in patients with acute coronary syndrome by 64-slice computed tomography. JACC Cardiovasc Imaging 2009;2:153-60.
35. Motoyama S, Kondo T, Sarai M, et al. Multislice computed tomographic characteristics of coronary lesions in acute coronary syndromes. J Am Coll Cardiol 2007;50:319-26.
36. Marwan M, Taher MA, El Meniawy K, et al. In vivo CT detection of lipid-rich coronary artery atherosclerotic plaques using quantitative histogram analysis: a head to head comparison with IVUS. Atherosclerosis 2011;215:110-5.
37. Achenbach S, Boehmer K, Pflederer T, et al. Influence of slice thickness and reconstruction kernel on the computed tomographic attenuation of coronary atherosclerotic plaque. J Cardiovasc Comput Tomogr 2010;4:110-5.
38. Dalager MG, Bottcher M, Dalager S, et al. Imaging atherosclerotic plaques by cardiac computed tomography in vitro: impact of contrast type and acquisition protocol. Invest Radiol 2011;46:790-5.
39. Tanami Y, Ikeda E, Jinzaki M, et al. Computed tomographic attenuation value of coronary atherosclerotic plaques with different tube voltage: an ex vivo study. J Comput Assist Tomogr 2010;34:58-63.
40. Cademartiri F, Mollet NR, Runza G, et al. Influence of intracoronary attenuation on coronary plaque measurements using multislice computed tomography: observations in an ex vivo model of coronary computed tomography angiography. Eur Radiol 2005;15:1426-31.
41. Cademartiri F, La Grutta L, Runza G, et al. Influence of convolution filtering on coronary plaque attenuation values: observations in an ex vivo model of multislice computed tomography coronary angiography. Eur Radiol 2007;17:1842-9.
42. Maurovich-Horvat P, Hoffmann U, Vorpahl M, et al. The napkin-ring sign: CT signature of high-risk coronary plaques? JACC Cardiovasc Imaging 2010;3:440-4.
43. Maurovich-Horvat P, Ferencik M, Voros S, et al. Comprehensive plaque assessment by coronary CT angiography. Nat Rev Cardiol 2014;11:390-402.
44. Maurovich-Horvat P, Schlett CL, Alkadhi H, et al. The napkin-ring sign indicates advanced atherosclerotic lesions in coronary CT angiography. JACC Cardiovasc Imaging 2012;5:1243-52.
45. Seifarth H, Schlett CL, Nakano M, et al. Histopathological correlates of the napkin-ring sign plaque in coronary CT angiography. Atherosclerosis 2012;224:90-6.
46. Puchner SB, Liu T, Mayrhofer T, et al. High-risk plaque detected on coronary CT angiography predicts acute coronary syndromes independent of significant stenosis in acute chest pain: results from the ROMICAT-II trial. J Am Coll Cardiol 2014;64:684-92.
47. Kashiwagi M, Tanaka A, Shimada K, et al. Distribution, frequency and clinical implications of napkin-ring sign assessed by multidetector computed tomography. J Cardiol 2013;61:399-403.
48. Otsuka K, Fukuda S, Tanaka A, et al. Napkin-ring sign on coronary CT angiography for the prediction of acute coronary syndrome. JACC Cardiovasc Imaging 2013;6:448-57.
49. Feuchtner G, Kerber J, Burghard P, et al. The high-risk criteria low-attenuation plaque <60 HU and the napkin-ring sign are the most powerful predictors of MACE: a long-term follow-up study. Eur Heart J Cardiovasc Imaging 2017;18:772-9.
50. Karanasos A, Ligthart JM, Witberg KT, et al. Calcified nodules: an underrated mechanism of coronary thrombosis? JACC Cardiovasc Imaging 2012;5:1071-2.
51. Burke AP, Farb A, Malcom GT, et al. Coronary risk factors and plaque morphology in men with coronary disease who died suddenly. N Engl J Med 1997;336:1276-82.
52. Farb A, Tang AL, Burke AP, et al. Sudden coronary death. Frequency of active coronary lesions, inactive coronary lesions, and myocardial infarction. Circulation 1995;92:1701-9.
53. Burke AP, Weber DK, Kolodgie FD, et al.

Pathophysiology of calcium deposition in coronary arteries. Herz 2001;26:239-44.
54. Huang H, Virmani R, Younis H, et al. The impact of calcification on the biomechanical stability of atherosclerotic plaques. Circulation 2001;103:1051-6.
55. Maldonado N, Kelly-Arnold A, Vengrenyuk Y, et al. A mechanistic analysis of the role of microcalcifications in atherosclerotic plaque stability: potential implications for plaque rupture. Am J Physiol Heart Circ Physiol 2012;303:H619-28.
56. Motoyama S, Sarai M, Harigaya H, et al. Computed tomographic angiography characteristics of atherosclerotic plaques subsequently resulting in acute coronary syndrome. J Am Coll Cardiol 2009;54:49-57.
57. van Velzen JE, de Graaf FR, de Graaf MA, et al. Comprehensive assessment of spotty calcifications on computed tomography angiography: comparison to plaque characteristics on intravascular ultrasound with radiofrequency backscatter analysis. J Nucl Cardiol 2011;18:893-903.
58. Kim SY, Kim KS, Seung MJ, et al. The culprit lesion score on multi-detector computed tomography can detect vulnerable coronary artery plaque. Int J Cardiovasc Imaging 2010;26:245-52.
59. Otsuka F, Finn AV, Virmani R. Do vulnerable and ruptured plaques hide in heavily calcified arteries? Atherosclerosis 2013;229:34-7.
60. Dweck MR, Chow MW, Joshi NV, et al. Coronary arterial 18F-sodium fluoride uptake: a novel marker of plaque biology. J Am Coll Cardiol 2012;59:1539-48.
61. Glagov S, Weisenberg E, Zarins CK, et al. Compensatory enlargement of human atherosclerotic coronary arteries. N Engl J Med 1987;316:1371-5.
62. Varnava AM, Mills PG, Davies MJ. Relationship between coronary artery remodeling and plaque vulnerability. Circulation 2002;105:939-43.
63. Achenbach S, Ropers D, Hoffmann U, et al. Assessment of coronary remodeling in stenotic and nonstenotic coronary atherosclerotic lesions by multidetector spiral computed tomography. J Am Coll Cardiol 2004;43:842-7.
64. Gauss S, Achenbach S, Pflederer T, et al. Assessment of coronary artery remodelling by dual-source CT: a head-to-head comparison with intravascular ultrasound. Heart 2011;97:991-7.
65. Motoyama S, Sarai M, Narula J, et al. Coronary CT angiography and high-risk plaque morphology. Cardiovasc Interv Ther 2013;28:1-8.
66. Arbab-Zadeh A, Fuster V. The myth of the "vulnerable plaque": transitioning from a focus on individual lesions to atherosclerotic disease burden for coronary artery disease risk assessment. J Am Coll Cardiol 2015;65:846-55.
67. Libby P, Pasterkamp G. Requiem for the 'vulnerable plaque'. Eur Heart J 2015;36:2984-7.
68. Kubo T, Maehara A, Mintz GS, et al. The dynamic nature of coronary artery lesion morphology assessed by serial virtual histology intravascular ultrasound tissue characterization. J Am Coll Cardiol 2010;55:1590-7.
69. Stone GW, Maehara A, Lansky AJ, et al. A prospective natural-history study of coronary atherosclerosis. N Engl J Med 2011;364:226-35.
70. Hlatky MA, Douglas PS, Cook NL, et al. Future directions for cardiovascular disease comparative effectiveness research: report of a workshop sponsored by the National Heart, Lung, and Blood Institute. J Am Coll Cardiol 2012;60:569-80.
71. Leipsic J, Abbara S, Achenbach S, et al. SCCT guidelines for the interpretation and reporting of coronary CT angiography: a report of the Society of Cardiovascular Computed Tomography Guidelines Committee. J Cardiovasc Comput Tomogr 2014;8:342-58.
72. Min JK, Shaw LJ, Devereux RB, et al. Prognostic value of multidetector coronary computed tomographic angiography for prediction of all-cause mortality. J Am Coll Cardiol 2007;50:1161-70.
73. Dedic A, Genders TS, Ferket BS, et al. Stable angina pectoris: head-to-head comparison of prognostic value of cardiac CT and exercise testing. Radiology 2011;261:428-36.
74. Andreini D, Pontone G, Mushtaq S, et al. A long-term prognostic value of coronary CT angiography in suspected coronary artery disease. JACC Cardiovasc Imaging 2012;5:690-701.
75. Pontone G, Andreini D, Bartorelli AL, et al. A long-term prognostic value of CT angiography and exercise ECG in patients with suspected CAD. JACC Cardiovasc Imaging 2013;6:641-50.
76. Nakazato R, Arsanjani R, Achenbach S, et al. Age-related risk of major adverse cardiac event risk and coronary artery disease extent and severity by coronary CT angiography: results from 15 187 patients from the International Multisite CONFIRM Study. Eur Heart J Cardiovasc Imaging 2014;15:586-94.
77. Cho I, Shim J, Chang HJ, et al. Prognostic value of multidetector coronary computed tomography angiography in relation to exercise electrocardiogram in patients with suspected coronary artery disease. J Am Coll

Cardiol 2012;60:2205-15.
78. Min JK, Koo BK, Erglis A, et al. Effect of image quality on diagnostic accuracy of noninvasive fractional flow reserve: results from the prospective multicenter international DISCOVER-FLOW study. J Cardiovasc Comput Tomogr 2012;6:191-9.
79. Pijls NH, Fearon WF, Tonino PA, et al. Fractional flow reserve versus angiography for guiding percutaneous coronary intervention in patients with multivessel coronary artery disease: 2-year follow-up of the FAME (Fractional Flow Reserve Versus Angiography for Multivessel Evaluation) study. J Am Coll Cardiol 2010;56:177-84.
80. Tonino PA, Fearon WF, De Bruyne B, et al. Angiographic versus functional severity of coronary artery stenoses in the FAME study fractional flow reserve versus angiography in multivessel evaluation. J Am Coll Cardiol 2010;55:2816-21.
81. Kobayashi Y, Nam CW, Tonino PA, et al. The Prognostic Value of Residual Coronary Stenoses After Functionally Complete Revascularization. J Am Coll Cardiol 2016;67:1701-11.
82. Taylor CA, Fonte TA, Min JK. Computational fluid dynamics applied to cardiac computed tomography for noninvasive quantification of fractional flow reserve: scientific basis. J Am Coll Cardiol 2013;61:2233-41.
83. Nørgaard BL, Leipsic J, Gaur S, et al. Diagnostic performance of noninvasive fractional flow reserve derived from coronary computed tomography angiography in suspected coronary artery disease: the NXT trial (Analysis of Coronary Blood Flow Using CT Angiography: Next Steps). J Am Coll Cardiol 2014;63:1145-55.
84. Douglas PS, Pontone G, Hlatky MA, et al. Clinical outcomes of fractional flow reserve by computed tomographic angiography-guided diagnostic strategies vs. usual care in patients with suspected coronary artery disease: the prospective longitudinal trial of FFR(CT): outcome and resource impacts study. Eur Heart J 2015;36:3359-67.
85. Hlatky MA, De Bruyne B, Pontone G, et al. Quality-of-Life and Economic Outcomes of Assessing Fractional Flow Reserve With Computed Tomography Angiography: PLATFORM. J Am Coll Cardiol 2015;66:2315-23.
86. Douglas PS, De Bruyne B, Pontone G, et al. 1-Year Outcomes of FFRCT-Guided Care in Patients With Suspected Coronary Disease: The PLATFORM Study. J Am Coll Cardiol 2016;68:435-45.
87. Coenen A, Lubbers MM, Kurata A, et al. Fractional flow reserve computed from noninvasive CT angiography data: diagnostic performance of an on-site clinician-operated computational fluid dynamics algorithm. Radiology 2015;274:674-83.
88. De Geer J, Sandstedt M, Bjorkholm A, et al. Software-based on-site estimation of fractional flow reserve using standard coronary CT angiography data. Acta Radiol 2016;57:1186-92.
89. Coenen A, Lubbers MM, Kurata A, et al. Coronary CT angiography derived fractional flow reserve: Methodology and evaluation of a point of care algorithm. J Cardiovasc Comput Tomogr 2016;10:105-13.
90. Yang DH, Kim YH, Roh JH, et al. Diagnostic performance of on-site CT-derived fractional flow reserve versus CT perfusion. Eur Heart J Cardiovasc Imaging 2017;18:432-40.
91. Choi JH, Min JK, Labounty TM, et al. Intracoronary transluminal attenuation gradient in coronary CT angiography for determining coronary artery stenosis. JACC Cardiovasc Imaging 2011;4:1149-57.
92. Wong DT, Ko BS, Cameron JD, et al. Transluminal attenuation gradient in coronary computed tomography angiography is a novel noninvasive approach to the identification of functionally significant coronary artery stenosis: a comparison with fractional flow reserve. J Am Coll Cardiol 2013;61:1271-9.
93. Ko BS, Wong DT, Norgaard BL, et al. Diagnostic Performance of Transluminal Attenuation Gradient and Noninvasive Fractional Flow Reserve Derived from 320-Detector Row CT Angiography to Diagnose Hemodynamically Significant Coronary Stenosis: An NXT Substudy. Radiology 2016;279:75-83.
94. Nakanishi R, Matsumoto S, Alani A, et al. Diagnostic performance of transluminal attenuation gradient and fractional flow reserve by coronary computed tomographic angiography (FFR(CT)) compared to invasive FFR: a sub-group analysis from the DISCOVER-FLOW and DeFACTO studies. Int J Cardiovasc Imaging 2015;31:1251-9.
95. Ko BS, Wong DT, Cameron JD, et al. The ASLA Score: A CT Angiographic Index to Predict Functionally Significant Coronary Stenoses in Lesions with Intermediate Severity-Diagnostic Accuracy. Radiology 2015;276:91-101.
96. Graham MM, Faris PD, Ghali WA, et al. Validation of three myocardial jeopardy scores in a population-based cardiac catheterization cohort. Am Heart J 2001;142:254-61.
97. Caruso D, Eid M, Schoepf UJ, et al. Dynamic CT myocardial perfusion imaging. Eur J Radiol

2016;85:1893-9.
98. Mancini GB, Hartigan PM, Shaw LJ, et al. Predicting outcome in the COURAGE trial (Clinical Outcomes Utilizing Revascularization and Aggressive Drug Evaluation): coronary anatomy versus ischemia. JACC Cardiovasc Interv 2014;7:195-201.
99. Dougoud S, Fuchs TA, Stehli J, et al. Prognostic value of coronary CT angiography on long-term follow-up of 6.9 years. Int J Cardiovasc Imaging 2014;30:969-76.
100. Al-Mallah MH. Does coronary CT angiography improve risk stratification over coronary artery calcium scoring in symptomatic patients with a low pre-test probability of coronary artery disease and a CAC of zero? Reply. Eur Heart J Cardiovasc Imaging 2014;15:232-3.
101. Min JK, Dunning A, Lin FY, et al. Age- and sex-related differences in all-cause mortality risk based on coronary computed tomography angiography findings results from the International Multicenter CONFIRM (Coronary CT Angiography Evaluation for Clinical Outcomes: An International Multicenter Registry) of 23,854 patients without known coronary artery disease. J Am Coll Cardiol 2011;58:849-60.
102. Lin FY, Shaw LJ, Dunning AM, et al. Mortality risk in symptomatic patients with nonobstructive coronary artery disease: a prospective 2-center study of 2,583 patients undergoing 64-detector row coronary computed tomographic angiography. J Am Coll Cardiol 2011;58:510-9.
103. Mark DB, Nelson CL, Califf RM, et al. Continuing evolution of therapy for coronary artery disease. Initial results from the era of coronary angioplasty. Circulation 1994;89:2015-25.
104. Miller JM, Rochitte CE, Dewey M, et al. Diagnostic performance of coronary angiography by 64-row CT. N Engl J Med 2008;359:2324-36.
105. Expert Panel on Detection, Evaluation, and Treatment of High Blood Cholesterol in Adults. Executive Summary of The Third Report of The National Cholesterol Education Program (NCEP) Expert Panel on Detection, Evaluation, And Treatment of High Blood Cholesterol In Adults (Adult Treatment Panel III). JAMA 2001;285:2486-97.
106. Wilson PW, D'Agostino RB, Levy D, et al. Prediction of coronary heart disease using risk factor categories. Circulation 1998;97:1837-47.
107. Austen WG, Edwards JE, Frye RL, et al. A reporting system on patients evaluated for coronary artery disease. Report of the Ad Hoc Committee for Grading of Coronary Artery Disease, Council on Cardiovascular Surgery, American Heart Association. Circulation 1975;51:5-40.
108. CONFIRM risk calculator. Cited February 28, 2016. Available online: http://www.ctconfirm.org/risk/
109. Kalbfleisch H, Hort W. Quantitative study on the size of coronary artery supplying areas postmortem. Am Heart J 1977;94:183-8.
110. Leaman DM, Brower RW, Meester GT, et al. Coronary artery atherosclerosis: severity of the disease, severity of angina pectoris and compromised left ventricular function. Circulation 1981;63:285-99.
111. de Araújo Gonçalves P, Garcia-Garcia HM, Dores H, et al. Coronary computed tomography angiography-adapted Leaman score as a tool to noninvasively quantify total coronary atherosclerotic burden. Int J Cardiovasc Imaging 2013;29:1575-84.
112. Chow BJ, Small G, Yam Y, et al. Incremental prognostic value of cardiac computed tomography in coronary artery disease using CONFIRM: COroNary computed tomography angiography evaluation for clinical outcomes: an InteRnational Multicenter registry. Circ Cardiovasc Imaging 2011;4:463-72.
113. Mushtaq S, De Araujo Gonçalves P, Garcia-Garcia HM, et al. Long-term prognostic effect of coronary atherosclerotic burden: validation of the computed tomography-Leaman score. Circ Cardiovasc Imaging 2015;8:e002332.
114. Serruys PW, Morice MC, Kappetein AP, et al. Percutaneous coronary intervention versus coronary-artery bypass grafting for severe coronary artery disease. N Engl J Med 2009;360:961-72.
115. Serruys PW, Unger F, van Hout BA, et al. The ARTS study (Arterial Revascularization Therapies Study). Semin Interv Cardiol 1999;4:209-19.
116. Ryan TJ, Faxon DP, Gunnar RM, et al. Guidelines for percutaneous transluminal coronary angioplasty. A report of the American College of Cardiology/American Heart Association Task Force on Assessment of Diagnostic and Therapeutic Cardiovascular Procedures (Subcommittee on Percutaneous Transluminal Coronary Angioplasty). Circulation 1988;78:486-502.
117. Hamburger JN, Serruys PW, Scabra-Gomes R, et al. Recanalization of total coronary occlusions using a laser guidewire (the European TOTAL Surveillance Study). Am J Cardiol 1997;80:1419-23.
118. Topol EJ. Textbook of interventional cardiology. 4th ed. Philadelphia: Saunders, 2003.
119. Lefèvre T, Louvard Y, Morice MC, et al. Stenting of bifurcation lesions: classification, treatments, and results. Catheter Cardiovasc Interv 2000;49:274-83.

120. Suh YJ, Hong YJ, Lee HJ, et al. Prognostic value of SYNTAX score based on coronary computed tomography angiography. Int J Cardiol 2015;199:460-6.
121. Farooq V, van Klaveren D, Steyerberg EW, et al. Anatomical and clinical characteristics to guide decision making between coronary artery bypass surgery and percutaneous coronary intervention for individual patients: development and validation of SYNTAX score II. Lancet 2013;381:639-50.
122. Furlow B. Radiation dose in computed tomography. Radiol Technol 2010;81:437-50.
123. Brenner DJ, Hall EJ. Computed tomography--an increasing source of radiation exposure. N Engl J Med 2007;357:2277-84.
124. Wang CL, Cohan RH, Ellis JH, et al. Frequency, management, and outcome of extravasation of nonionic iodinated contrast medium in 69,657 intravenous injections. Radiology 2007;243:80-7.
125. Federle MP, Chang PJ, Confer S, et al. Frequency and effects of extravasation of ionic and nonionic CT contrast media during rapid bolus injection. Radiology 1998;206:637-40.
126. Nadjiri J, Hausleiter J, Jahnichen C, et al. Incremental prognostic value of quantitative plaque assessment in coronary CT angiography during 5 years of follow up. J Cardiovasc Comput Tomogr 2016;10:97-104.
127. van Rosendael AR, Kroft LJ, Broersen A, et al. Relation between quantitative coronary CTA and myocardial ischemia by adenosine stress myocardial CT perfusion. J Nucl Cardiol 2016. [Epub ahead of print].
128. Tesche C, De Cecco CN, Caruso D, et al. Coronary CT angiography derived morphological and functional quantitative plaque markers correlated with invasive fractional flow reserve for detecting hemodynamically significant stenosis. J Cardiovasc Comput Tomogr 2016;10:199-206.
129. Tesche C, Plank F, De Cecco CN, et al. Prognostic implications of coronary CT angiography-derived quantitative markers for the prediction of major adverse cardiac events. J Cardiovasc Comput Tomogr 2016;10:458-65.
130. Gillies RJ, Kinahan PE, Hricak H. Radiomics: Images Are More than Pictures, They Are Data. Radiology 2016;278:563-77.
131. Kolossváry M, Kellermayer M, Merkely B, et al. Cardiac Computed Tomography Radiomics A Comprehensive Review on Radiomic Techniques. J Thorac Imaging 2017. [Epub ahead of print].
132. Davnall F, Yip CS, Ljungqvist G, et al. Assessment of tumor heterogeneity: an emerging imaging tool for clinical practice? Insights Imaging 2012;3:573-89.
133. O'Connor JP, Rose CJ, Waterton JC, et al. Imaging intratumor heterogeneity: role in therapy response, resistance, and clinical outcome. Clin Cancer Res 2015;21:249-57.

Cite this article as: Kolossváry M, Szilveszter B, Merkely B, Maurovich-Horvat P. Plaque imaging with CT—a comprehensive review on coronary CT angiography based risk assessment. Cardiovasc Diagn Ther 2017;7(5):489-506. doi: 10.21037/cdt.2016.11.06

